Final Report

The Development of the ASPS Vernier System

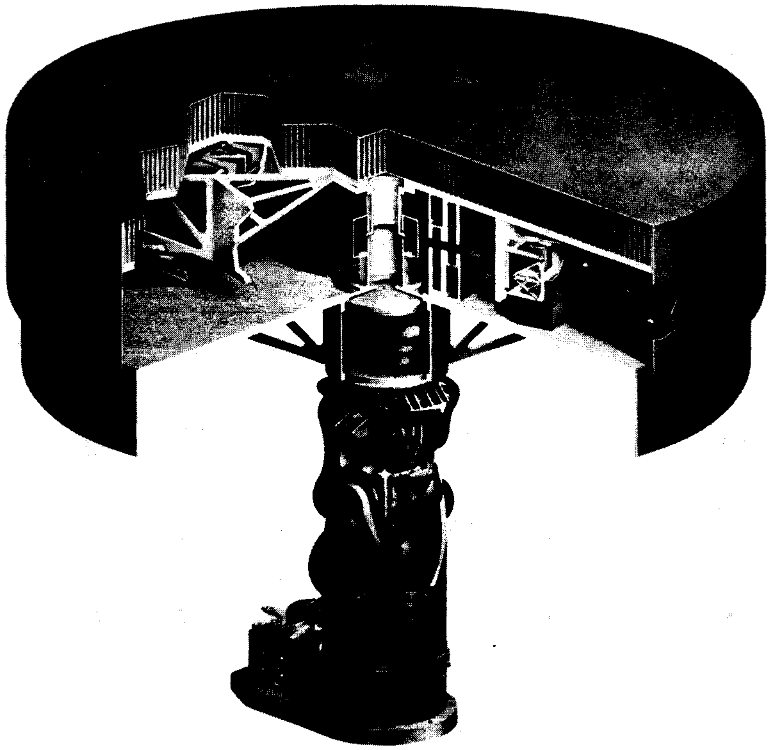

SPERRY CORPORATION
FLIGHT SYSTEMS
PHOENIX, AZ 85036

CONTRACT NO. NAS1-15008
JUNE 1983

NASA

National Aeronautics and
Space Administration

Langley Research Center
Hampton, Virginia 23665

(NASA-CR-183224) THE DEVELOPMENT OF THE ASPS VERNIER SYSTEM Final Report (Sperry Corp.) 37 p

N89-70006

Unclas
00/35 0121598

Final Report

The Development of the ASPS Vernier System

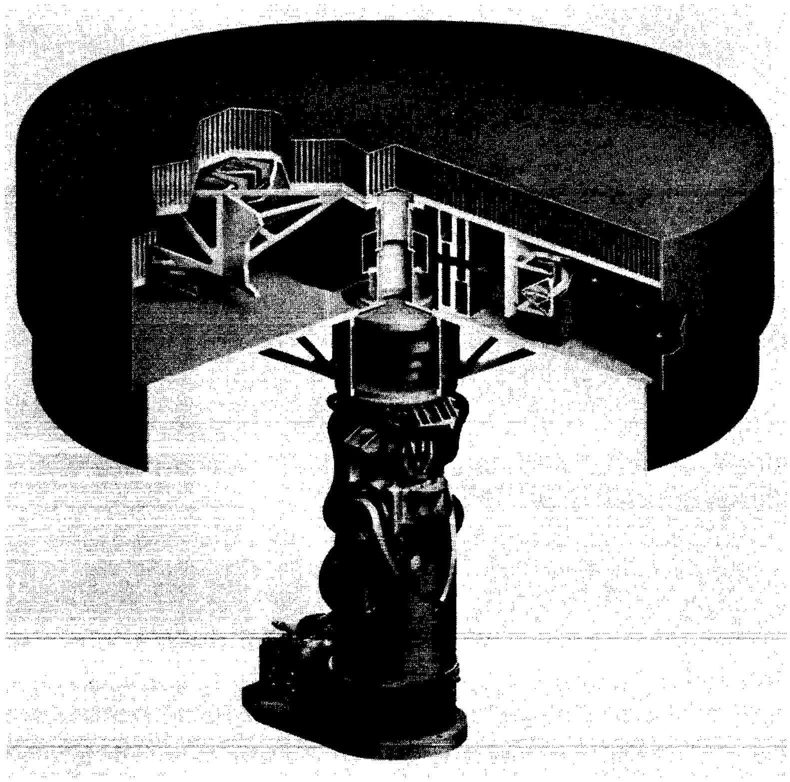

5-15845

SPERRY CORPORATION
FLIGHT SYSTEMS
PHOENIX, AZ 85036

CONTRACT NO. NAS1-15008
JUNE 1983

NASA

National Aeronautics and
Space Administration

Langley Research Center
Hampton, Virginia 23665

TABLE OF CONTENTS

LIST OF ILLUSTRATIONS

LIST OF TABLES

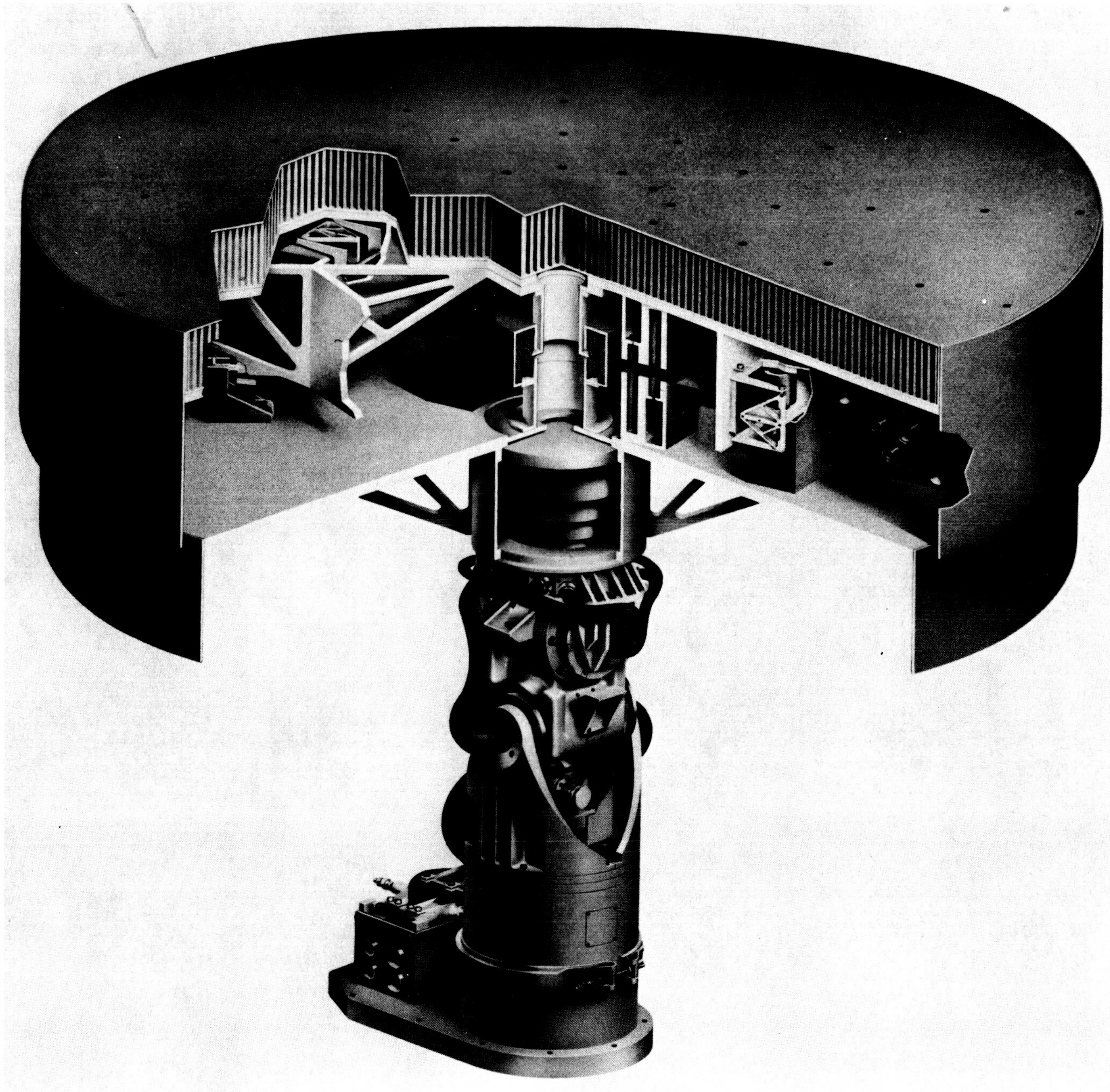

5-15845

Figure 1
ASPS Configuration

FINAL REPORT:
THE DEVELOPMENT OF THE ASPS VERNIER SYSTEM

Brian J. Hamilton
Flight Systems, Sperry Corporation

SUMMARY

The Annular Suspension and Pointing System (ASPS) is an end-mount experiment pointing system designed for use in the Space Shuttle. This report describes the development of the ASPS Vernier System (AVS), the noncontacting magnetic suspension module of the ASPS which provides for fine pointing (.01 arcsecond) of a payload and isolation from carrier disturbances and flexible modes. An artist's conception of this system is shown in Figure 1.

The AVS development program has been funded by the NASA Langley Research Center since mid-1976. Six years later, all major aspects of the technology have been demonstrated in the laboratory. In addition, this technology is being incorporated into an Air Force flight program. NASA continues to fund related development activities such as the means of providing services to the payload across a noncontacting interface.

The scope of this document is to provide a general description of the technology, its background, evolution, and status. The breadth of technical information pertinent to the AVS development is too great to allow coverage here in depth. Instead, a complete list of references is included to allow the interested reader to pursue specific subjects in greater depth. The more important references are mentioned in the text of this report.

ACRONYMS

AGS	ASPS Gimbal System
ASPS	Annular Suspension and Pointing System
AVS	ASPS Vernier System
CG	Center of Gravity
DOF	Degrees of Freedom
MBA	Magnetic Bearing Assembly
MBPS	Megabit Per Second
MSFC	Marshall Space Flight Center
NASA	National Aeronautics and Space Administration
SOT	Solar Optical Telescope

INTRODUCTION AND BACKGROUND

During the past decade, firm definitions have emerged for many of the payloads destined for flight on the Space Shuttle. An Experiment Pointing Mount Working Group was formed by the NASA to examine the requirements of these payloads. The results of this investigation clearly indicated a need for an auxiliary pointing system capable of subarcsecond performance. This performance must be maintained for extended periods (1 hour) in the carrier vehicle disturbance environment, consisting of both vibrational (cooling pumps) and transient (man-motion and vernier thruster firings) disturbances. In mid-1976, Sperry Flight Systems was awarded a contract by the NASA Langley Research Center to develop a system, known as the Annular Suspension and Pointing System (ASPS),[1, 3, 5], capable of .01 arcsecond stability. This system consists of a modular gimbal set to which is attached a magnetically levitated isolation and vernier pointing system. This effort has produced engineering models of both systems which have been subjected to extensive laboratory evaluations. This newly developed technology is applicable to a wide range of missions, both free-flying and shuttle-borne, particularly those involving high-resolution optics.

In order to understand why a pointing system which includes magnetic suspension exhibits superior pointing performance, it is first important to understand why conventional pointing systems do not. A conventional pointing system, for purposes of this discussion, is one which constrains the relative motion between payload and carrier to only rotational degrees of freedom. The axes about which these rotations occur are referred to as gimbal axes, and they are fixed in both payload and carrier body-fixed coordinates. At these axes, the payload must translate as the carrier translates, and the gimbal bearings will apply forces to the payload as necessary to achieve this objective. Given vibrations and transient disturbances on the carrier body, the pointed payload will be continually subjected to disturbance forces in three axes by the gimbal bearings. These forces, under all but ideal conditions, will result in pointing disturbances.

Steps can be taken to reduce these pointing disturbances. First, the torques which result from the bearing forces can be reduced by diminishing the offset between the gimbal axes and the payload center of mass. This is the CG-mount approach, illustrated in Figure 2a. This configuration has been used for years, and minimizes the adverse effects of fixed gimbal axes. Because large gimbal bearing forces are applied, sensitivity is very high to slight motions of the CG due to expendables, or slight errors in coalignment of gimbal axes and CG. Furthermore, the center of mass of many payloads is not conveniently accessible as an attachment point, thus the pointing system must surround the payload. This makes it cumbersome and difficult to standardize since it must be custom-designed to fit around each payload. Finally, multiaxis systems become cumbersome indeed, since all gimbal axes must intersect at the payload center of mass.

A more convenient geometry locates the gimbal axes at the base of the payload. This configuration is called end-mount pointing, and is illustrated in Figure 2b.

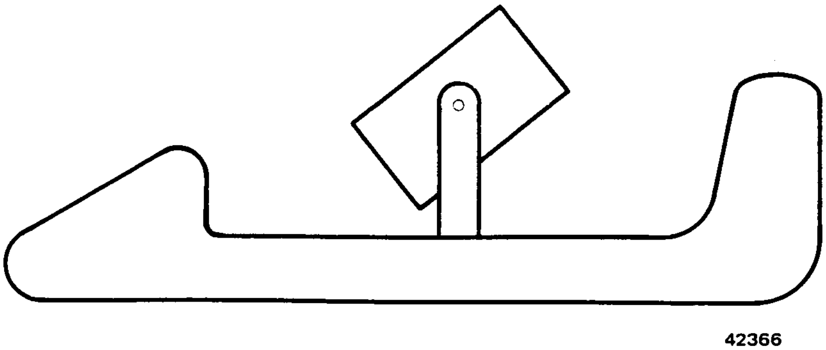

Figure 2a
CG-Mount Pointing

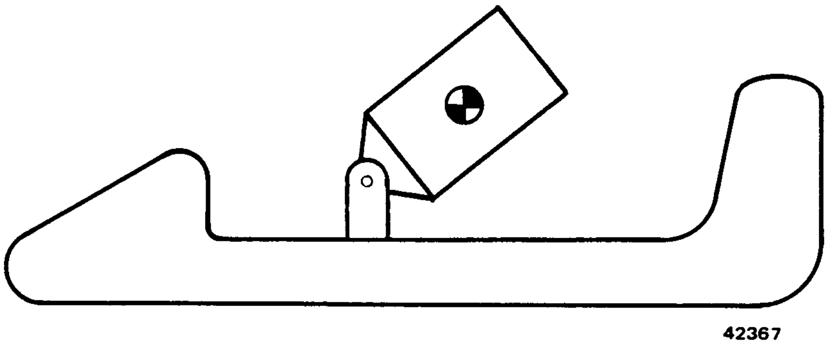

Figure 2b
End-Mount Pointing

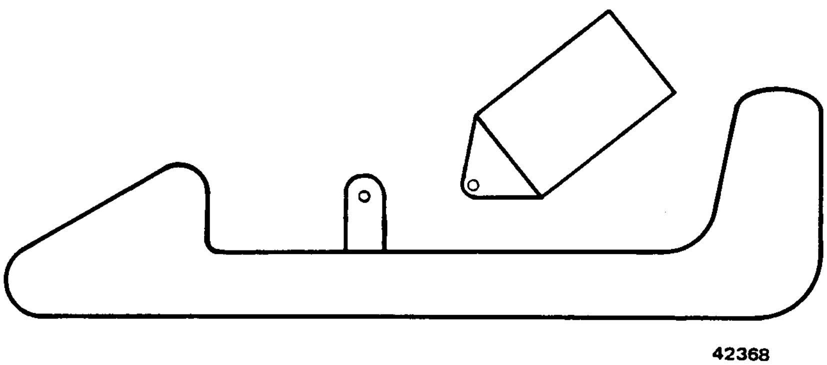

Figure 2c
Isolation

Figure 2
Mount Pointing System Configuration

Many of the disadvantages described above are alleviated by end-mount pointing, but the problem of coupling between translation and pointing remains, and must be dealt with. The effects of end-mount coupling can be reduced actively, to a certain extent. First, the bandwidth of the pointing servo loops could simply be increased until the necessary stiffness was obtained. This approach is limited by such factors as payload structural dynamics, sensor bandwidths, digital computation times, and excessive torquer requirements. Secondly, the carrier accelerations could be measured and torques fed open-loop to the gimbals to prevent overturning. This technique is more practical, and in fact, is used in the ASPS Gimbal System (AGS) when the vernier module is absent. However, this scheme also has practical limitations, particularly regarding torquer requirements and acceleration feedforward noise. In either case, the goal is to minimize pointing error about a rigid gimbal axis by making the payload translate with the carrier. Thus any vibrations on the carrier are transmitted to the payload, which may also be undesirable. Where high frequency vibrations are involved, neither technique is effective since the ability to cancel the error rolls off with the torquer frequency response.

All these difficulties are due to the fact that the payload is hard-mounted to the carrier through rigid gimbal axes. Clearly, a solution to the problem is to isolate the payload from the carrier in translation. For example, in the CG-mounted system, the high sensitivity to CG motion resulted from the large forces applied by stiff bearings. If those bearings could be made more compliant, it would follow that smaller forces would be applied to the payload, and thus sensitivity would be reduced. Of course, many orders of magnitude of stiffness reduction would be necessary, which is not realistic for conventional bearings. As the bearing stiffness is reduced, it becomes both possible and necessary for the payload to translate with respect to the carrier, thus introducing three more degrees of freedom which had been hitherto constrained. In fact, as the translation stiffness is reduced further, the payload begins to act as though it were a free body no longer attached to the carrier at all, and able to move in fully six degrees of freedom. This phenomenon is referred to as isolation. As the translation stiffness is reduced to zero, complete isolation is achieved. Here the payload is truly a free flyer, and does not respond at all to carrier disturbances. Unfortunately, it does not stay aboard the carrier either, but instead drifts away, out of control (Figure 2c).

A practical high performance pointing system should have the ability to provide a high degree of isolation, but still constrain payload motion to only a few millimeters from the carrier. It should be noncontacting for long life and minimal nonlinearity, and should, therefore, employ noncontacting actuators to apply forces and torques in six degrees of freedom to the constrained free-flying payload. It should be end-mounted for operational flexibility, but must not suffer degraded performance due to end-mount coupling. This outline of an elegant approach to stable pointing is, in fact, a good description of a magnetic suspension.

Figure 3 indicates some typical vibration transfer functions, as derived and discussed in Reference 14. Note that a magnetic suspension takes best advantage of both the pointing loop attenuation and the translation loop rolloff.

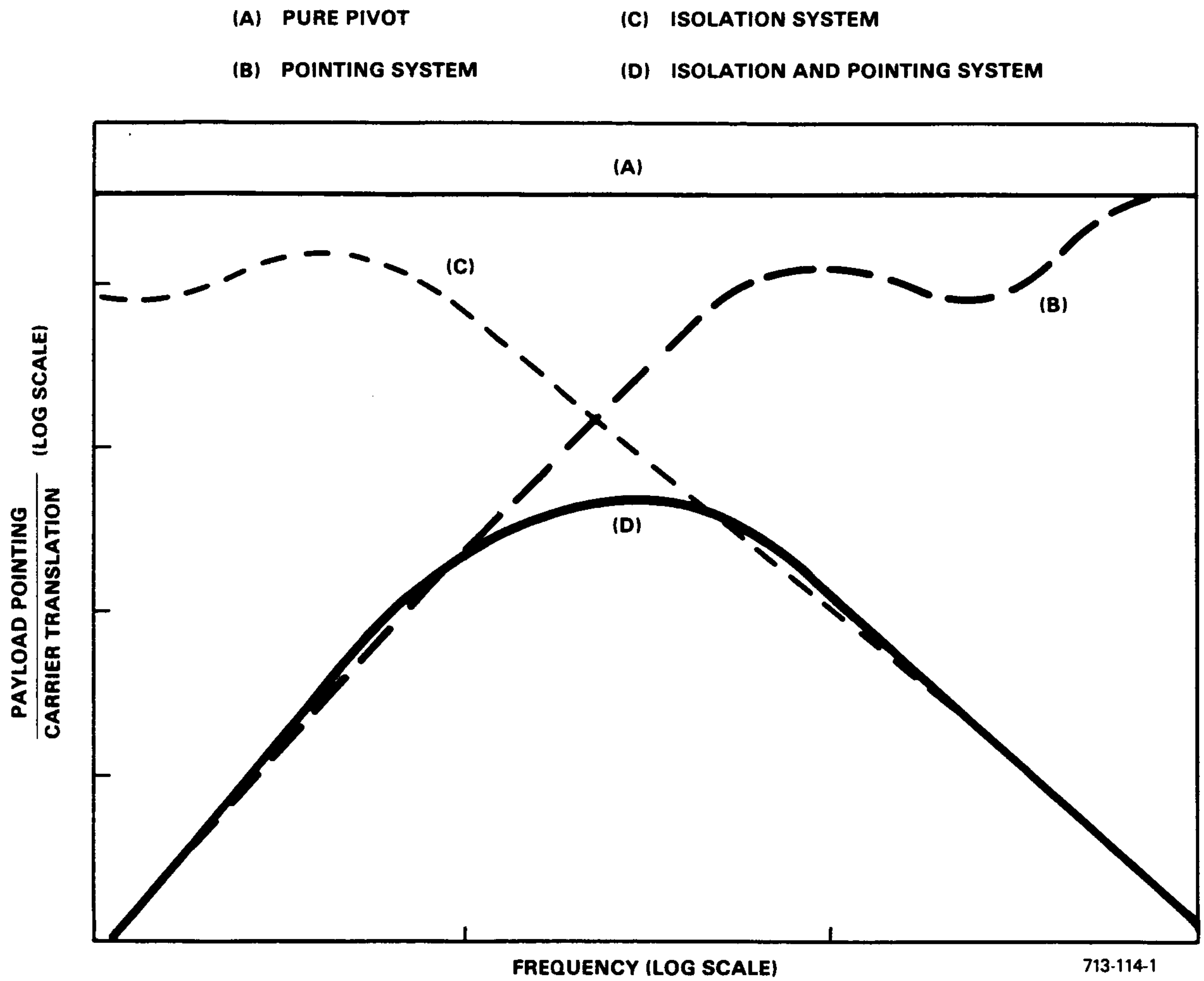

Figure 3
Generic System Vibration Transfer Functions

SYSTEM DESCRIPTION

The ASPS Vernier System (AVS) consists of six Magnetic Bearing Assemblies (MBAs), each of which is capable of applying a precisely known force to the levitated body while allowing substantial relative motion in any axis. The combined effect of these six forces is the ability to control all six degrees of freedom (DOF) of the body.

Figures 4a and 4b show the radial locations of the six magnetic actuators. Note that there are three MBAs oriented so that the applied force is out of the page, and three more whose force vectors are tangent to the MBA circle. These are referred to as axial MBAs and tangential MBAs, respectively. By using these actuators in sum and difference combinations, forces and torques can be applied to provide 6 DOF control of the levitated payload.

Each magnetic bearing assembly (Figure 5) consists of rotor and stator halves. The rotor half is attached to the payload and the stator half is mounted on the carrier side, at the top of the gimbal stack. The stator assembly includes magnetic coils to apply the force and a position sensor to measure rotor position in the magnetic gap. The rotor assembly consists of a magnetic iron rotor plate and a force sensor mechanism. The force sensor measures the force transmitted to the payload from the rotor plate.

The block diagram of Figure 6 shows the AVS control scheme. Note that position control is not exercised locally at each MBA, but instead a coordinate transformation to body axes is performed. In this way, control of translation can be separated from the control of rotation (pointing). Even though these loops share the same actuators, it is possible for them to have completely different bandwidths, dynamics, and feedback paths. The three translational degrees of freedom are controlled with extremely low bandwidth (typically .01 Hz to provide isolation), while pointing bandwidths are higher (typically 1.0 Hz), and are limited by payload structural dynamics. Similarly, translation loops are closed on a differential measurement between rotor and stator, while pointing loops are usually based on an inertial reference or star tracker on the levitated body. This provides optimal inertial pointing and minimal gap travel in translation. Since these control laws and transformations are implemented in software, suspension dynamics and axes of rotation can be selected at will, even in flight.

In-flight calibration can be performed on the decoupling matrices to ensure orthogonality between the six axes. By applying a fixed force command at each MBA in turn and observing the resultant payload accelerations in six DOF, the matrix can be derived. This process corrects for errors due to CM offset uncertainty, MBA scale factor, and location errors.

To maintain the isolation capability of the magnetic suspension requires that the power and data interfaces to the payload also be noncontacting. Optical data channels capable of 30 MBPS have been demonstrated which can accommodate the gap motions. Power is transferred using a special large air-gap ironless secondary transformer. While development of this transformer is not yet complete, it is continuing under NASA funding.

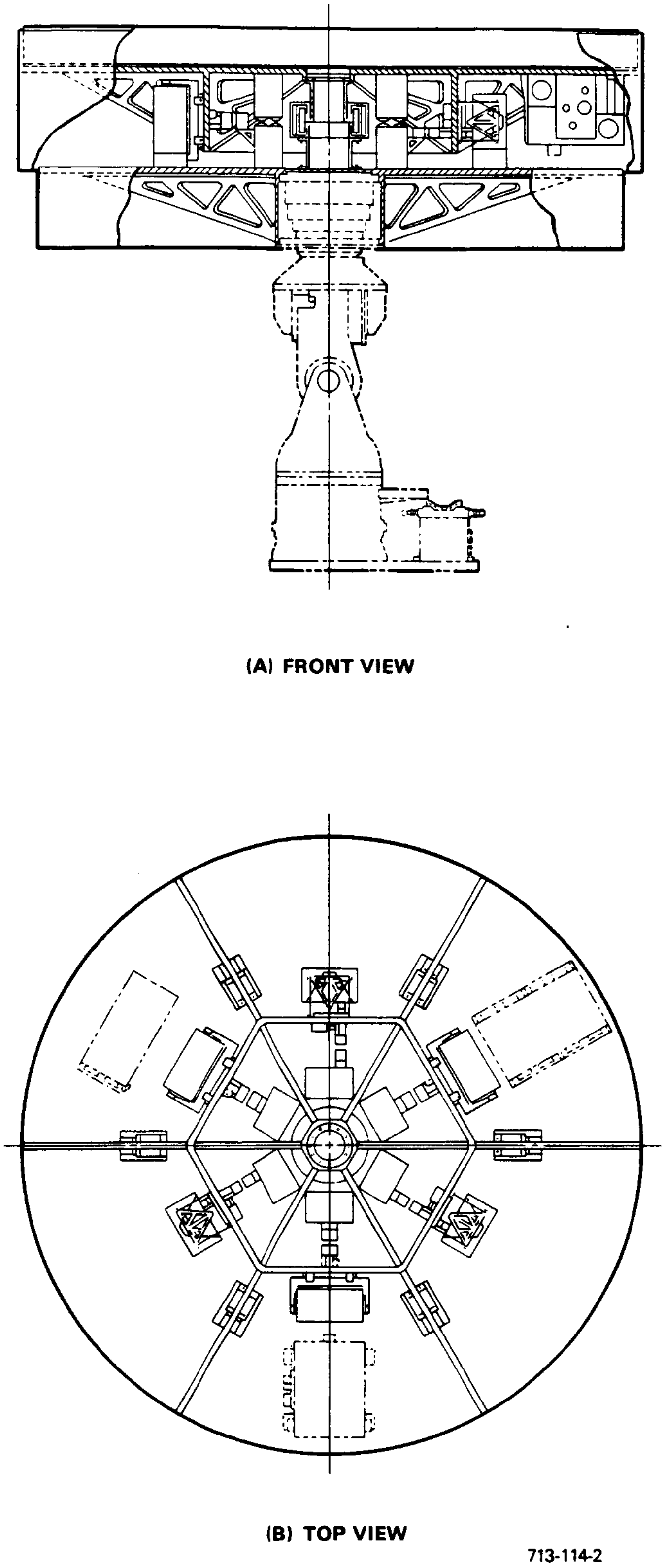

Figure 4
AVS Layout

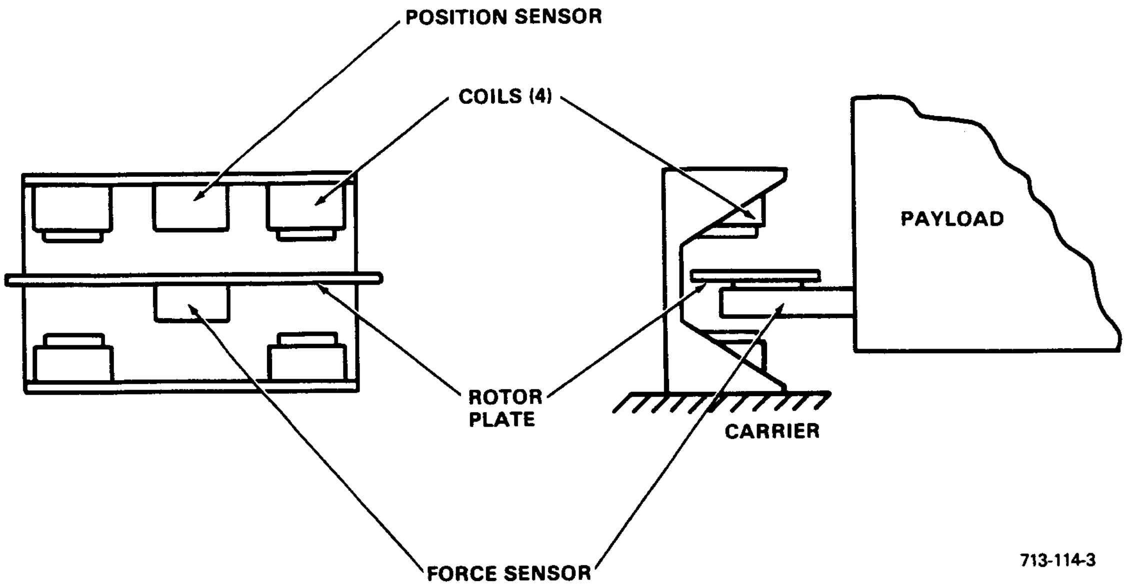

Figure 5
Magnetic Bearing Assembly (MBA)

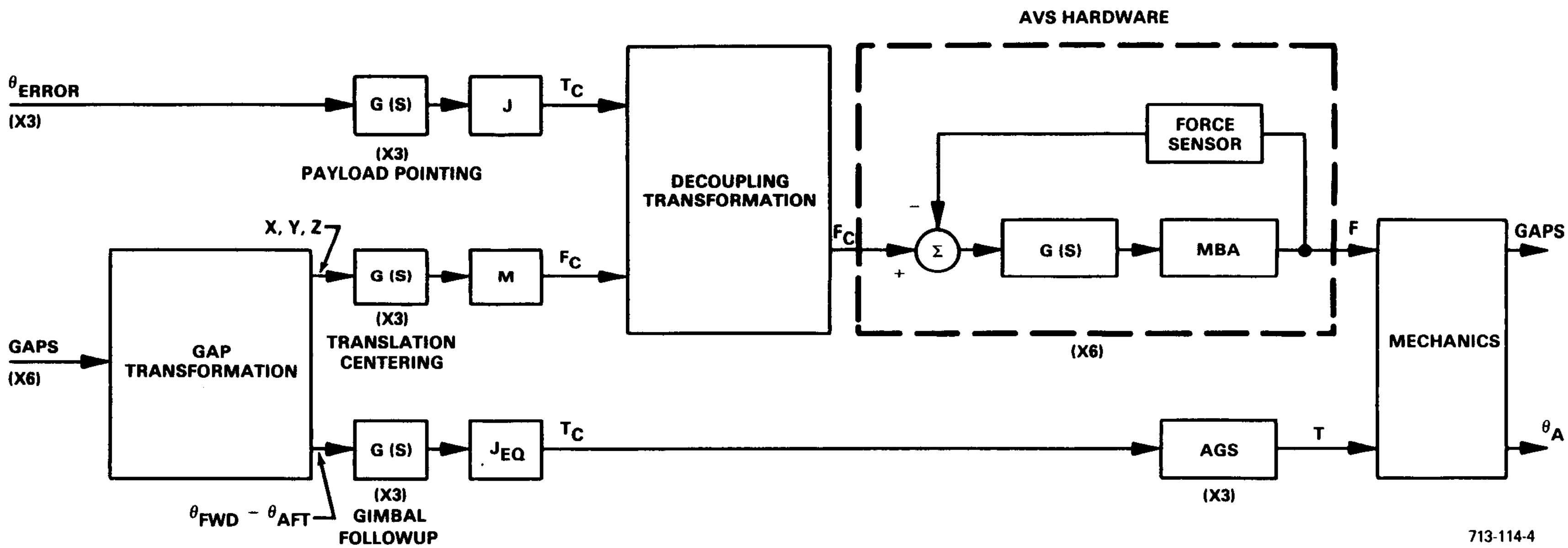

Figure 6
System Block Diagram

A summary of the ASPS characteristics and capabilities is shown in Table 1.

TABLE 1

ASPS CHARACTERISTICS

• Pointing Range	±.75 degree
• Pointing Stability*	.01 arcsecond
• Pointing Bandwidth (typical)	1.0 hertz
• Translation Bandwidth (typical)	.1 hertz
• Slew Rate	3 degree/second
• Payloads	
Mass	Up to 7200 kilograms
Mass-Inertia Ratio	Up to at least 1 m^{-2}
CG Offset	Up to 3 m
Size	Unconstrained, due to end-mounting
*During worst-case shuttle VRCS firing	

PERFORMANCE PREDICTIONS

The new AVS configuration was studied extensively by simulation to determine expected performance in the Shuttle environment. Statistical analyses were performed to define the sensitivity of all identifiably independent error sources. An error budget was established showing the significant contributors of error and their relative contributions (Reference 56). The error budget is shown in Table 2 for a normalized payload. The general conclusion is that the .01-arcsecond goal is achievable for a variety of practical payloads. While the system is not yet truly sensor limited, the Space Telescope inertial reference unit which provides position feedback is the biggest contributor to error on the list. Extrapolation to other payloads is shown in Figure 7. Note that a SOT-class payload would be in the flat section of the curve, indicating that performance is sensor-limited. Figure 7 would indicate that the SOT requirements are met even when using the production model DRIRU-II.

In addition to these rigid body analyses, some preliminary work has also been done in the area of flexibility analysis.[63] Preliminary findings indicate that, due to the noncontacting nature of magnetic suspension, the vernier control system is somewhat isolated from the bending modes of the gimbals and carrier beneath it. In addition, the gimbal dynamics are less impacted by the effects of payload modes.

TABLE 2

SYSTEM ERROR BUDGET[56] (EXCERPTS)

	Source	Error Factor	Effectiveness	Parameter Nominal Value			Expected Error	
				Mean	3σ	Units	Mean	3σ ($\widehat{\text{sec}}$)
Force Sensor	Scale Factor	$0.0094\sqrt{2}$ $\widehat{\text{sec}}$/%	0.10 ①	0	1	%	0	.00133
	Noise	0.71 $\widehat{\text{sec}}$/N rms	1.25 ④	0	.001	N rms	0	.00089
	Lag	0.223/fc $\widehat{\text{sec}}$	0.10 ②	100	0	Hz	.00022	0
	Hysteresis	0.018 $\widehat{\text{sec}}$/%	0.50 ②	0	.1	%	0	.00090
Position Sensor	Sampling	Nonlinear	1.00 ③	100	0	Hz	.00034	0
	Scale Factor	0.050/K_V $\widehat{\text{sec}}$/%	1.00 ③	0	1	%	0	.00039
	Bias	0.00134 $\widehat{\text{sec}}$/mm	1.00 ③	0	.5	mm	0	.00067
	Noise	25/K_V $\widehat{\text{sec}}$/mm rms	1.25 ④	0	.005	mm rms	0	.00104
	Lag	Nonlinear	1.00 ③	10	0	Hz	.00130	0
Force Actuator	Force Loop K_V Match	0.014/K_V $\widehat{\text{sec}}$/%	1.00 ③	5	0	%	.00047	0
	MBA Hysteresis	0.027/K_V $\widehat{\text{sec}}$/%	0.50 ②	1	4	%	.00009	.00036
Other AVS	MBA Radius Uncertainty	0.0094 $\widehat{\text{sec}}$/%	0.10 ①	0	.5	%	0	.00047
	ADS Stability	--	1.00 ③	0	$.3\Delta\theta q$	$\widehat{\text{sec}}$	0	.00011
AVS Total							.00242	.00233
Other	Payload CM Uncertainty	0.0094 $\widehat{\text{sec}}$/%	0.10 ①	0	3	%	0	.00282
	DRIRU Noise (Equivalent Angle)	single data point	1.25 ④	0	.0029	$\widehat{\text{sec}}$	0	.00363
	DRIRU Quantization	--	1.00 ③	.00036	0	$\widehat{\text{sec}}$	0	.00036
Total							.00242	.00516
	Flex Capsule	.0019 $\widehat{\text{sec}}$/N/m	.50	22	0	N/m	.02090	0

1 Error may be reduced by in-flight calibration procedures

2 Error tends to cancel when it exists in both axial and tangential sets

3 Error cannot be reduced

4 Noise sensitivities increased for conservative estimate

Conditions:

Normalized Payload $\frac{M}{J} = 1$

$m = 2000$ Kg $\quad J = \begin{bmatrix} 2000 & 0 & 0 \\ 0 & 2000 & 0 \\ 0 & 0 & 2000 \end{bmatrix}$

z offset = 1 m

VRCS Pitch Disturbance, Elevation Gimbal Angle = 1.5 rad

Control Loop Bandwidths: Gimbal 10 Hz, Pointing 1 Hz, Centering .1 Hz

Control Computation Rate: 100 Hz

Transport Delays: Force Commands 6 ms
Torque Commands 3 ms

Force Loop $K_I = 150$, $K_p = .25$, $K_V = K_I$

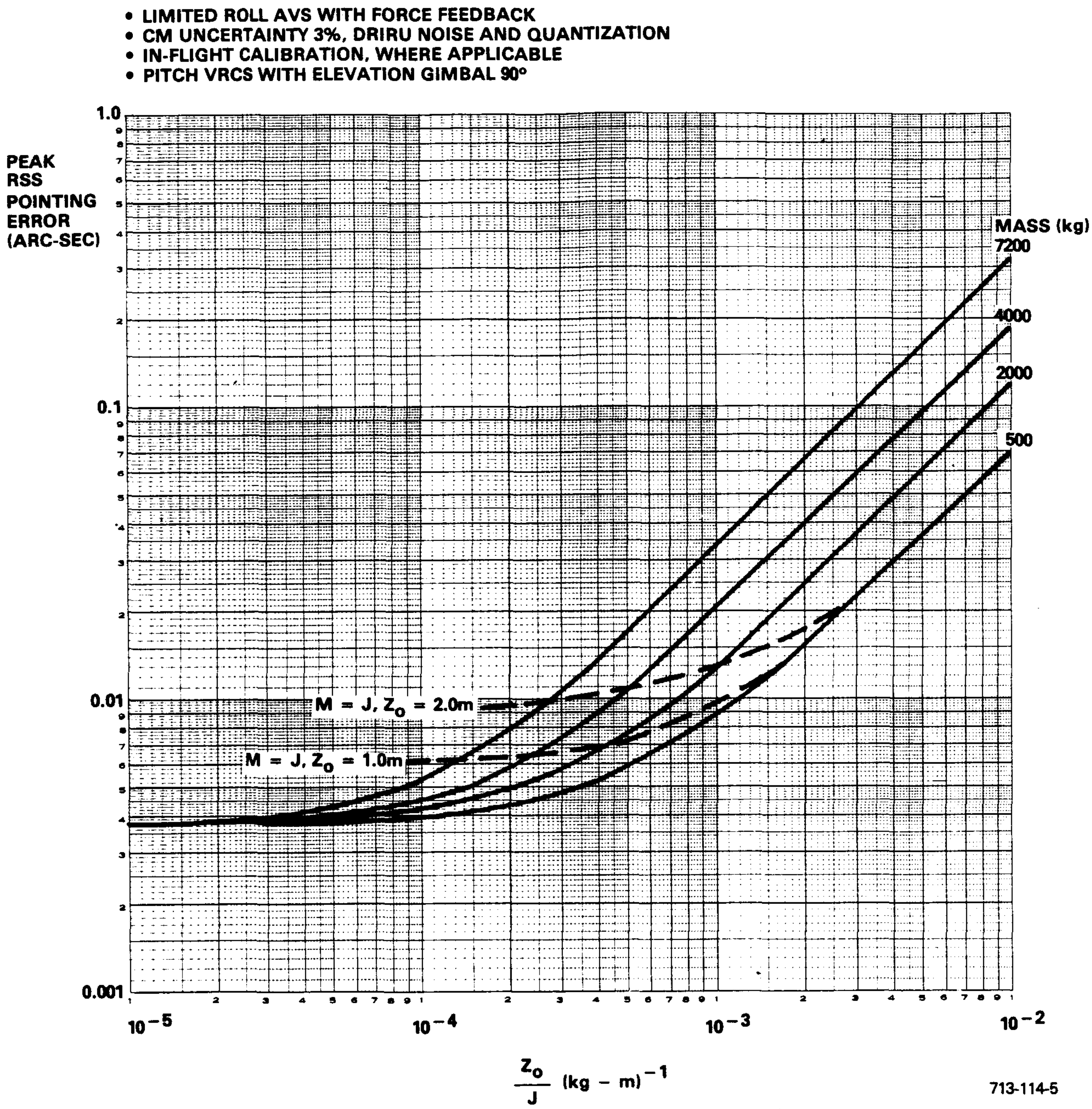

Figure 7
Performance Extrapolation[56]

EVOLUTION OF THE DESIGN

The ASPS was originally conceived at the NASA Langley Research Center[1]. In 1976, a contract was awarded to Sperry Flight Systems to design, fabricate, and test a protoflight ASPS. At this time the ASPS consisted of two gimbals (elevation and lateral) and a vernier system which provided unlimited freedom in the roll axis. The magnetic suspension was thus completely symmetric about the roll axis with all MBAs acting on an L-shaped annular homogeneous rotor. There were three axial MBAs, two radially directed MBAs, and a 200-hertz ac induction motor providing roll torque (Figure 8). The system design is described in the reference material, most notably Reference 10.

In late 1977, a two degree-of-freedom model of the magnetic suspension system was built and tested,[21] which consisted of two MBA stations acting on a single-motor section. This setup allowed control of one translation and one rotation DOF, thus allowing demonstration of the transformation and decoupling concepts used in the ASPS at a simple level. After successful completion of the 2 DOF testing, a protoflight 6 DOF build was begun.

As the program proceeded, it was decided to accelerate the development of the gimbal subsystem under a separate NASA-MSFC contract in order to satisfy early needs as forecasted by the experiment community. The remaining AVS program was perceived more as a technology advancement effort, and the protoflight hardware under construction was thus relaxed to the status of an engineering model.

Following engineering model fabrication, a year-long test sequence of this hardware was conducted. Figure 9 depicts the test facility, and Figure 10 shows the hardware with the laser interferometer which was used to assess performance. During this effort, it was discovered that the rotor position sensors were extremely temperature sensitive. In addition, if the cables to the transducer heads were moved, sensor calibration was seriously affected since cable capacitance was a part of the impedance bridge. As a corrective measure to these problems, temperature control was instituted in the test area, and the sensor cables were carefully secured in place. Force calibration was extremely tedious due to the difficulty in measuring force, and in the lack of repeatability resulting from hysteresis and nonconformance of the magnetic circuits to ideal laws. Nevertheless, after several iterations, force accuracy of 1 percent to 2 percent of full scale was achieved.[26,38]

With the closing of control loops came difficulties in sorting out the dynamics of the test fixture from the hardware under test. Significant advances were made in the zero-gravity suspension techniques employed, and after several modifications, the test fixture became sufficiently transparent in the data. Tests were performed on servo dynamics, decoupling control, stability during cross-axis disturbances, and a variety of other parameters (see references).

In order to validate the test results, a computer simulation was assembled. The dynamics of both the AVS and the test setup were modelled. All significant error sources (AVS and test equipment) were identified and included. Using the simulation, pointing sensitivity to each error source was obtained. These sensitivities were combined statistically to predict the mean and deviation of the pointing error during laboratory tests. Hardware test results within a three-sigma target area were considered successful. All control

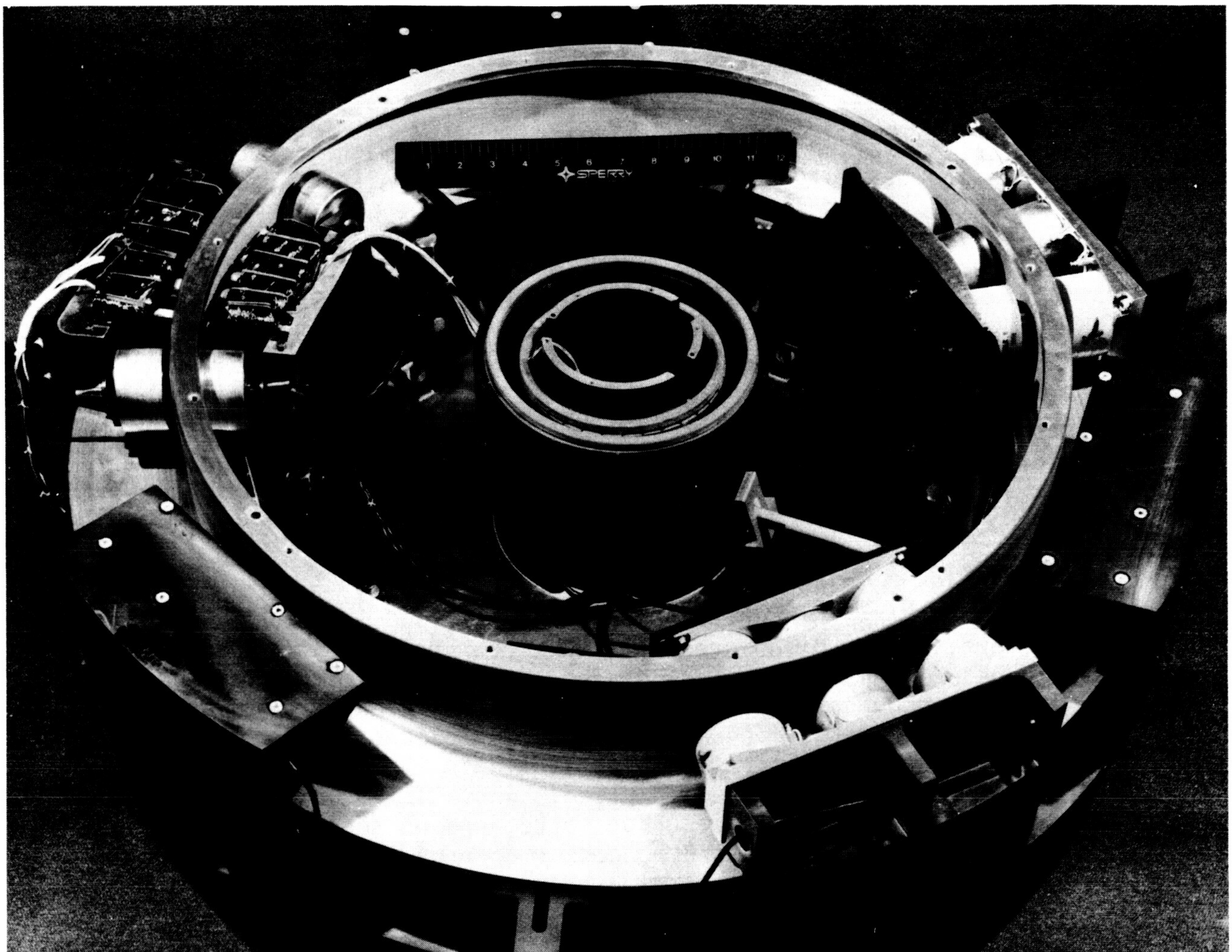

3-13066-3

Figure 8
AVS Engineering Model Hardware

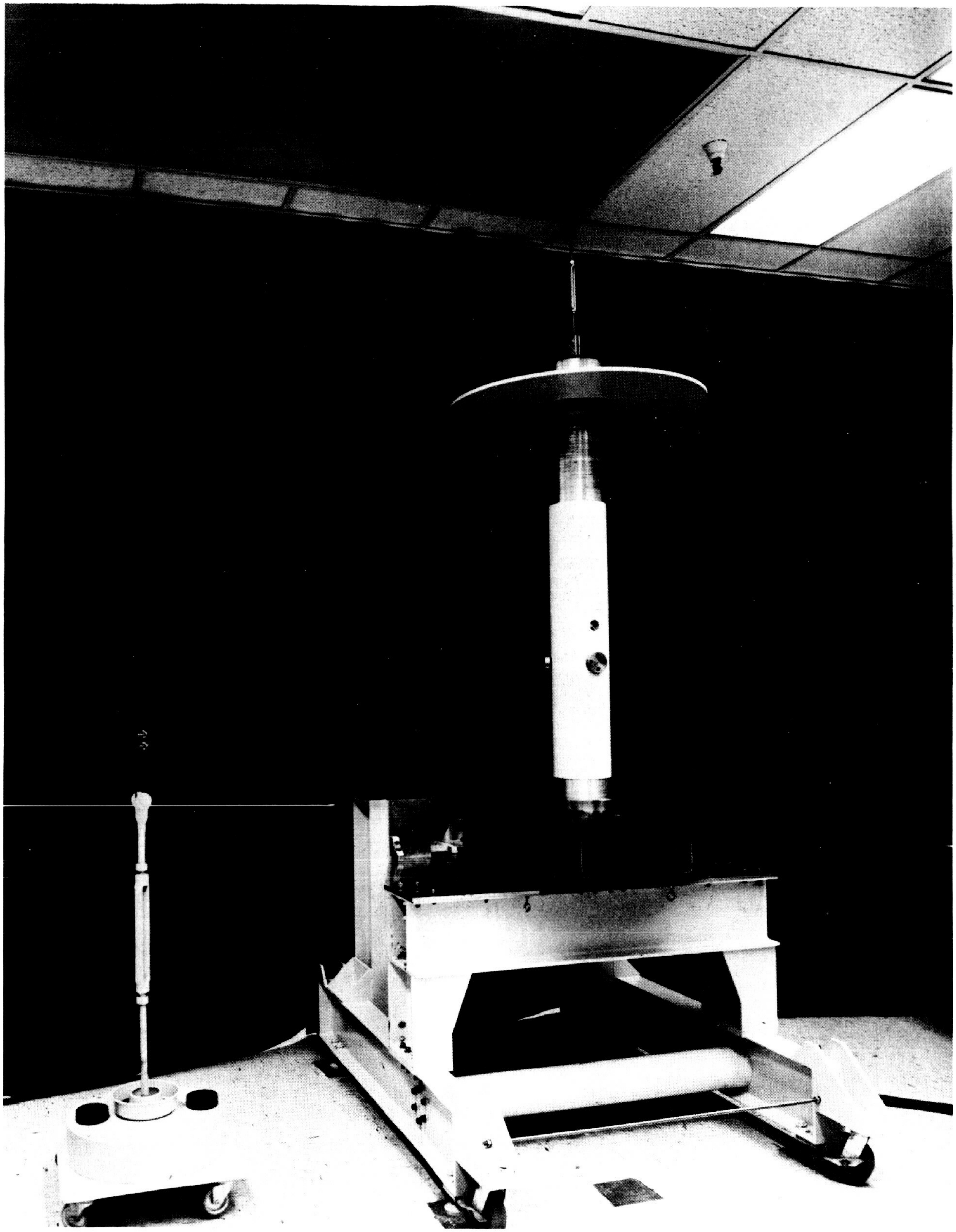

9-13680-3

Figure 9
Engineering Model Test Setup

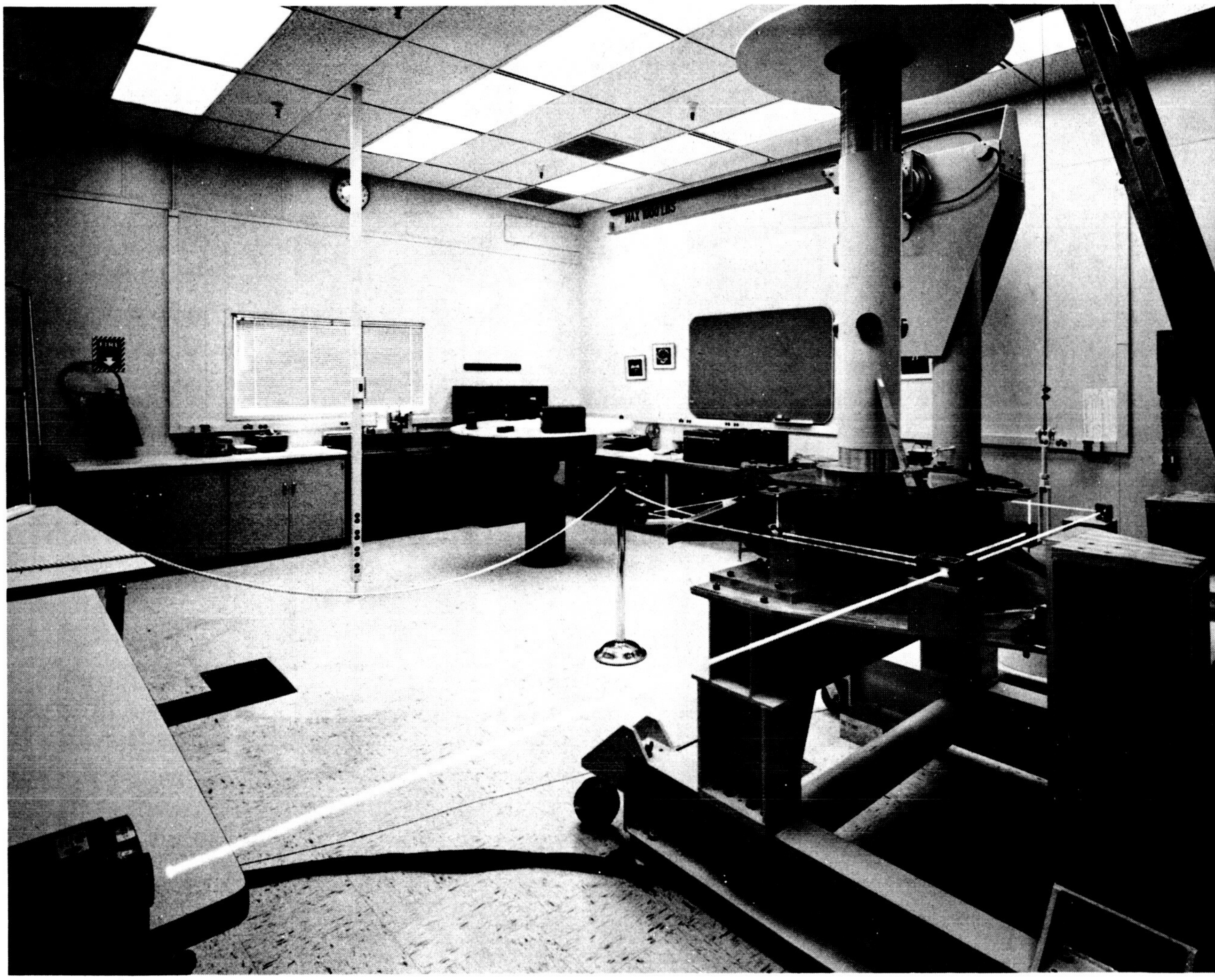

12-13782-1

Figure 10
Laser Interferometer

system parameters were computed prior to initiation of the laboratory tests. These parameters, which are based on payload mass, inertia, and CM location data, were computed in a manner identical to that required to support a Shuttle mission. The control system parameters were not empirically adjusted during tests since the test objective was to hit the predicted target and not to obtain best-possible laboratory performance. Likewise, control bandwidths were set to values proposed for use on orbit to maintain similarity between flight and laboratory systems.

In attempting to correlate test results with analytical predictions,[43,44] much was learned about system sensitivities and anomalies, which in turn permitted the refinement of analytical models. In general, good agreement was obtained between laboratory data and analytical predictions.[9] Stabilities in the range of .05 to .10 arcsecond were achieved even in the presence of test-fixture anomalies. Under nominal conditions, the mean and standard deviation of measured VRCS responses were 1.36 and .62 arcseconds, respectively, compared to simulation predicted values of 1.22 and .52. Although it was demonstrated by these tests that the decoupling control scheme was both effective and well understood, the data indicated that the quality of the magnetic actuators left something to be desired.

During this same time frame, NASA requested that the design be able to accommodate facility-class payloads with masses up to 7200 kg and inertias up to 40,000 kg-m^2. Analyses indicated that this was generally possible, but that the existing roll torque was inadequate by nearly an order of magnitude.[57] In addition, the unlimited roll concept as implemented in this AVS configuration afforded no practical backup alternatives for caging the payload in case of vernier system failure. Thus, at the conclusion of the test phase two major problems existed with the AVS design. First, the magnetic actuator performance was contributing too much to the error budget, and second, the roll axis torquer represented an operational deficiency and a performance uncertainty to this system.

The latter problem was solved first. In July 1979, MSFC directed Sperry to design and incorporate a roll-axis gimbal into the AGS system. This immediately provided for backup roll caging independent of the vernier. Of greater significance was the fact that it eliminated the requirement for unlimited roll freedom in the vernier module. This came at a time when the AVS program had just begun looking for ways to enhance the design and resolve the above-mentioned problems, so it wasn't long before the concept of a limited-roll vernier surfaced. The idea of a vernier roll axis has many advantages. First, pointing stability similar to pitch and yaw could now also be provided in roll. Second, the development and testing of the ac induction motor could be avoided by using a sixth MBA similar to the other five. This led to replacing the symmetric annular rotor with six separate rotor segments, one for each MBA. Manufacturing costs and weight were greatly reduced. In addition, available roll torque was increased over tenfold, as was roll efficiency. The new arrangement replaced the radial MBAs and roll motor with three identical tangential MBAs as shown in Figure 11. All six MBA stations could now be identical to reduce manufacturing costs.

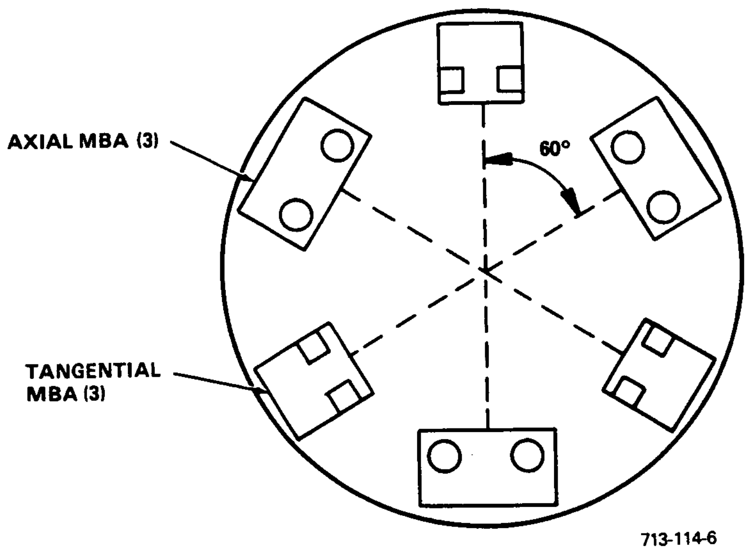

Figure 11
New MBA Arrangement

The new configuration was good in many ways, but it had not addressed the most serious design problem - MBA performance. The errors observed fell into two major categories: position sensor performance (for gap compensation) and magnetics performance (hysteresis, linearity, etc). As such, activities were initiated in the areas of position sensor improvement and hysteresis reduction. Many new options were now open for position sensing which had not been available in the unlimited roll configuration. With individual rotor segments, the sensor did not have to operate on a passive, homogeneous target. It was decided to pursue an optical position sensing concept based on a CCD array (Figure 12). A brassboard was built and tested with an accuracy of approximately 1 percent of full scale demonstrated and nearly an order of magnitude improvement predicted possible with more work. Further work has also been devoted to position sensing by Sperry Research Center.[64]

In the area of magnetic hysteresis reduction, several techniques were studied.[28,34,36,37,41] Pieces of material were subjected to more elaborate heat-treating procedures and retested. Superposition of ac degaussing current on top of the control currents was considered. It was concluded that some improvement was possible, but probably not enough. The prospects of marginal hysteresis performance, marginal position sensor performance, and complex open-loop calibrations led to a second assessment of the entire gap-compensation control scheme.

The true output of an MBA is force. Given the nonlinearities and anomalies of the magnetic circuit, it made sense to consider using feedback techniques to attenuate errors. Therefore, it was decided to attempt to close a force feedback loop around the MBA as a solution, not only to the magnetic anomalies, but to position sensor errors as well. The entire actuator, as then designed, would be placed in the forward path of the loop, and resultant static errors would be only those of the force sensor itself. Such a loop is depicted in Figure 13.

Analysis and simulation showed[54,56] that great performance improvements could be achieved in this manner. However, the required force sensor represented the state of the art in performance. High resolution, high bandwidth, high stiffness, low hysteresis, low noise, and low temperature coefficient all in a device which could survive the vibration environment seemed a virtually impossible request. Several technologies were studied, and a vibrating quartz sensor was ultimately selected for development. A subcontract was awarded to Quartex, Inc, of Salt Lake City, Utah, to develop a force sensor (Figure 14) to meet these requirements. As indicated in Table 3, the units delivered performed much better than required in all respects with one exception - stiffness. Stiffness will be addressed in future iterations, probably during the Air Force flight program development. The effect of finite stiffness on performance is that a resonance results from the stiffness of the sensor and mass of the rotor. This resonance complicates the stable design of the force loop. Nevertheless, it has been shown by analysis that the force loop is stable and improves system performance under typical conditions by two orders of magnitude. This is particularly the case for applications in which vibration isolation is essential.

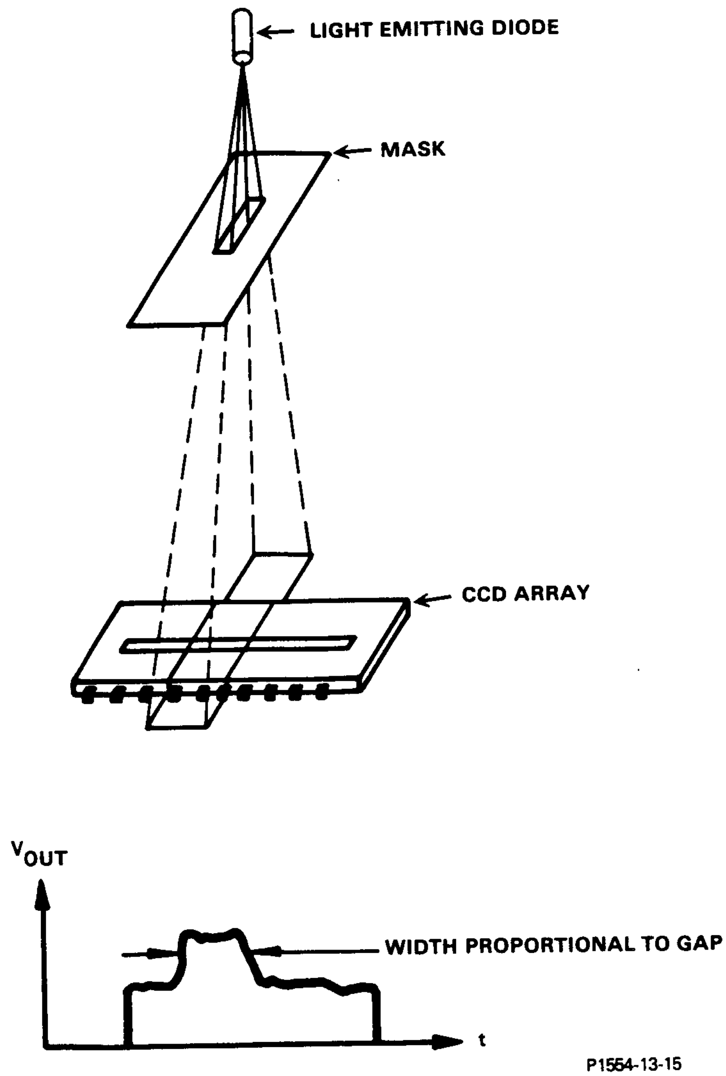

Figure 12
Optical Position Sensor Concept

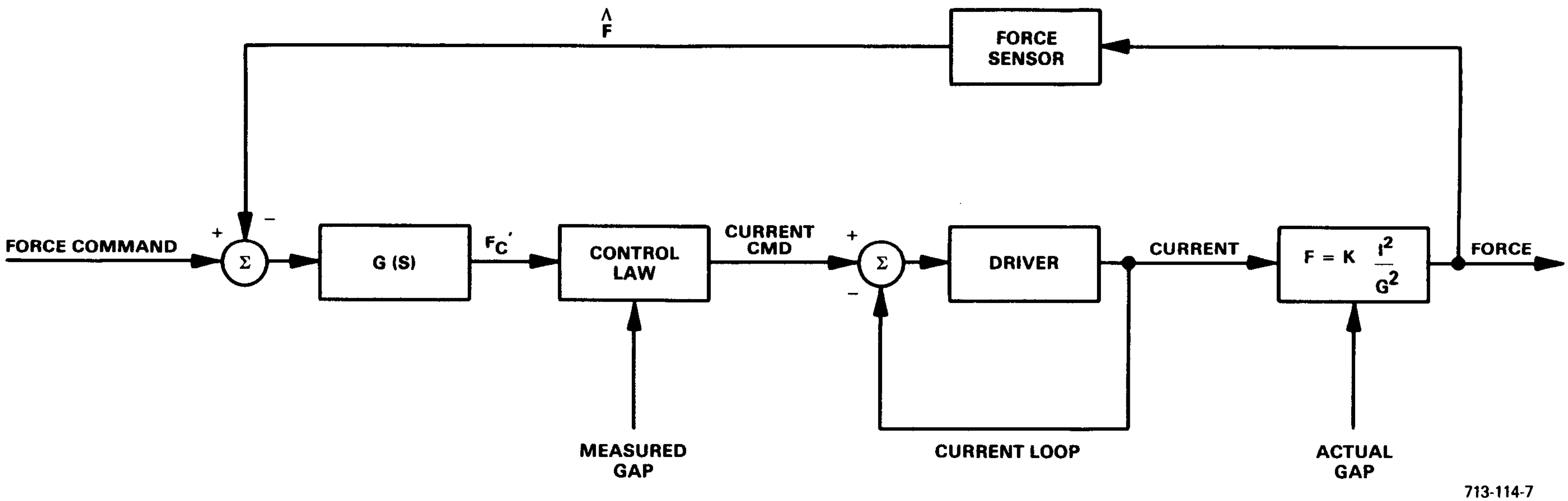

Figure 13
MBA Block Diagram

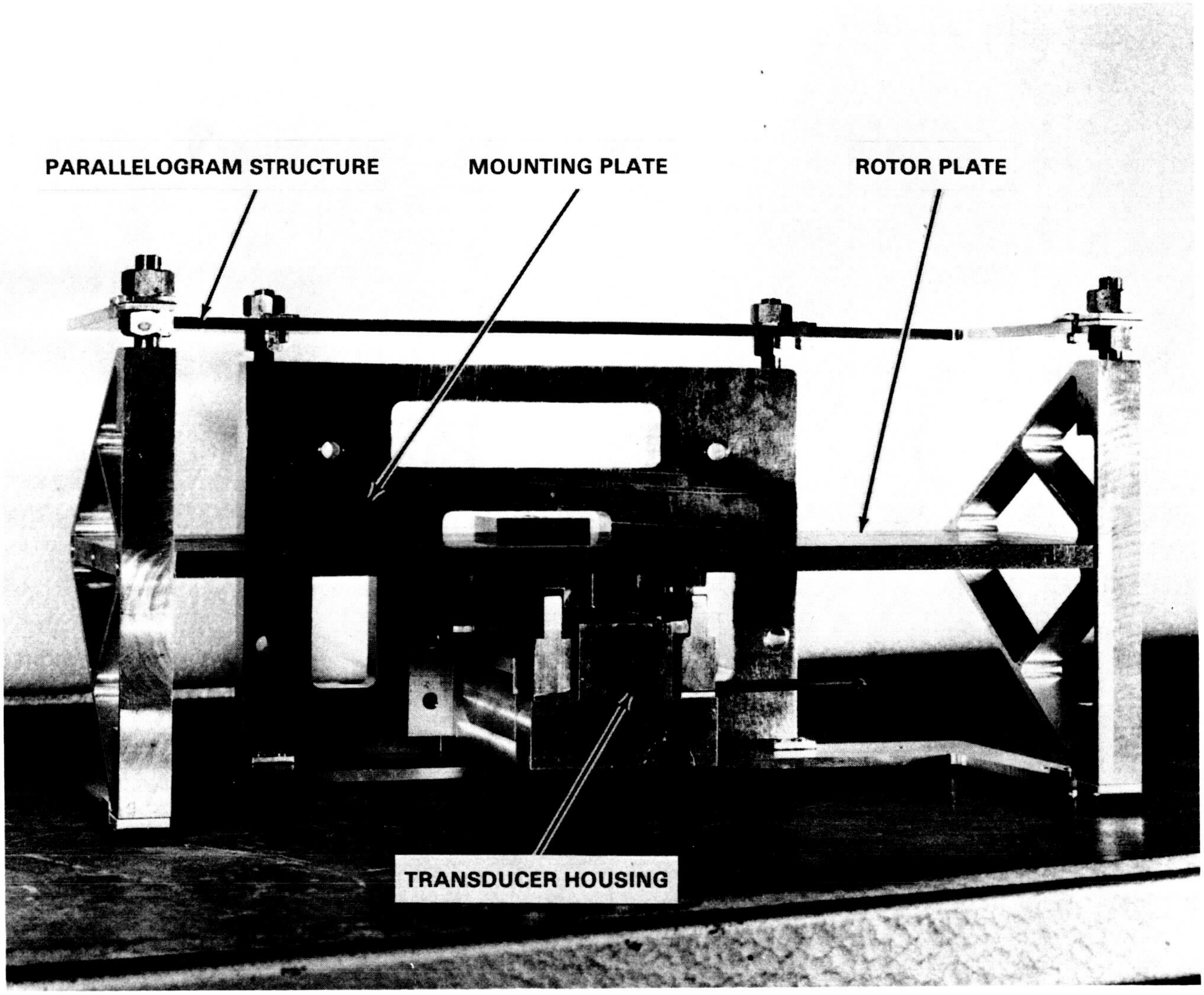

14-15511-1

Figure 14
Force Sensor Prototype

TABLE 3

FORCE SENSOR REQUIREMENTS AND PERFORMANCE[59]

Requirement	Specification	Actual
Range	±40 N	±40 N
Linearity	±.4 N	±.003 N
Offset no load zero shift	1.0 N	±.002 N
Offset Rate (at constant temperature and pressure)	.0005 N/s	7.0×10^{-7} N/s
Noise	.001 N	.0002 N
Resolution	.001 N	.0002 N
Hysteresis	.08 N	.002 N
Stiffness	6×10^{6} N/m	1.48×10^{4} N/m
Cross-Axis Sensitivity	±.04 N	±.002 N
Temperature Offset -20°C to 100°C	1.0 N	.55 N
Pressure offset 0 to 1 atm	1.0 N	.76 N

Recently, the concepts of the second generation AVS have been demonstrated in a single degree-of-freedom test fixture (Figure 15). These tests, referred to as the single station tests,[62] demonstrated the performance of a single MBA station when equipped with the force loop and optical gap sensor. A multiple degree-of-freedom demonstration was not required since the decoupling laws were adequately demonstrated with the earlier 5 DOF engineering model.

In summary, the current AVS design consists of six identical MBA stations, each having a rotor segment, force sensor, and optical gap sensor. This configuration is referred to as the second generation AVS (see Figure 1).

PERIPHERAL DEVELOPMENTS

Two significant peripheral technologies have been pursued as a part of the AVS development. These are the means for providing: (1) power, and (2) data across the noncontacting interface.

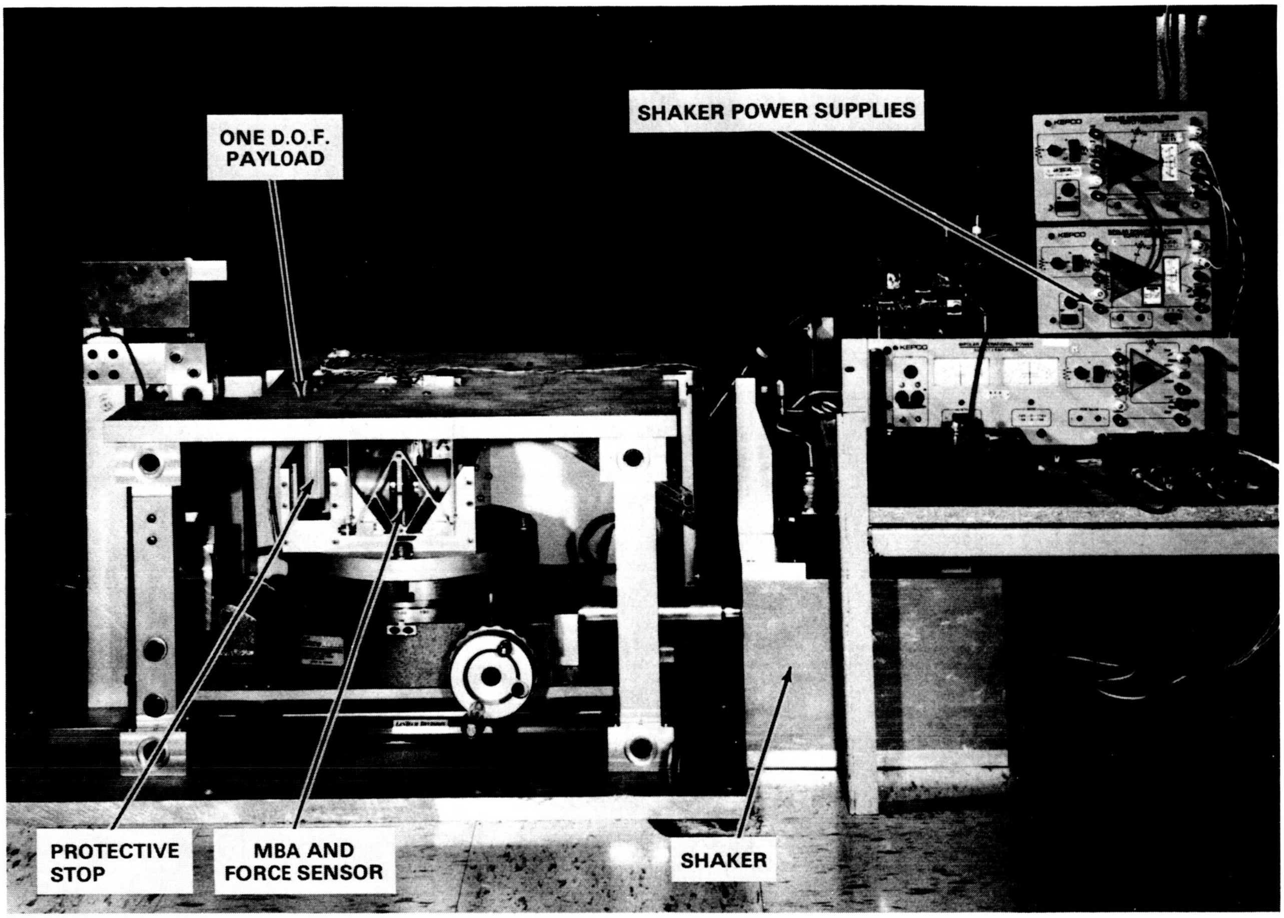

12-15549-3

Figure 15
Single-Station Test Setup

Power

The original ASPS concept included batteries on the levitated portion which were occasionally charged during inoperative periods. The many drawbacks of batteries, such as excessive weight, explosive chemical properties, limited temperature capabilities, etc, prompted a search for alternatives. At first, transformers were rejected because large magnetic forces would exist between primary and secondary, disturbing the magnetic suspension. Later, a concept surfaced in which these forces would be minimal. The key was removing all iron on the secondary side in favor of wraparound iron on the primary. Since the moving secondary is only a coil of wire and has little impact on the flux flow, no force is generated. This device is depicted in the center of Figure 4b. This concept is being pursued under NASA funding.

Data

Two-way multichannel digital communication is necessary to support virtually any payload which would be flown on the AVS. When the unlimited roll design was baselined, this was an extremely difficult task that resulted in a special cylindrically symmetric optical coupler design. However, now that differential motion is restricted everywhere within the vernier module, optical channels can be arranged easily in several places using much simpler optics. Figure 16 shows a typical lensing arrangement which makes reasonable signal-to-noise ratios possible despite the differential motion between bodies. Optical data links of up to 30 MBPS data rates have been demonstrated in the laboratory.[58] This technology is, therefore, considered in hand. Figure 4 depicts several optical channels in the toroidal area between the transformer and the MBAs.

CONCLUSIONS

The design of the magnetically suspended AVS has matured to a viable configuration for flight design which should be capable of attaining its specified performance in the presence of carrier disturbances. Preliminary studies indicate that it should simplify control system design in the presence of bending modes. The original technology depended upon precise and delicate calibrations of each component which could be neither verified nor corrected in flight, and which required accuracies pressing the state of the art of the magnetic bearings themselves. The second-generation design is simpler, easier to manufacture, and can be calibrated at the subassembly level as well as in flight. It has eliminated the need for such refinements as more accurate position sensing and hysteresis removal or cancellation. It is more efficient than its predecessor and able to meet the needs of facility class payloads. Its errors have been studied and performance predicted, and while it is not yet truly sensor-limited, the present rate sensor is the largest error in the budget. The technology developed under this effort is being incorporated into an Air Force flight program.

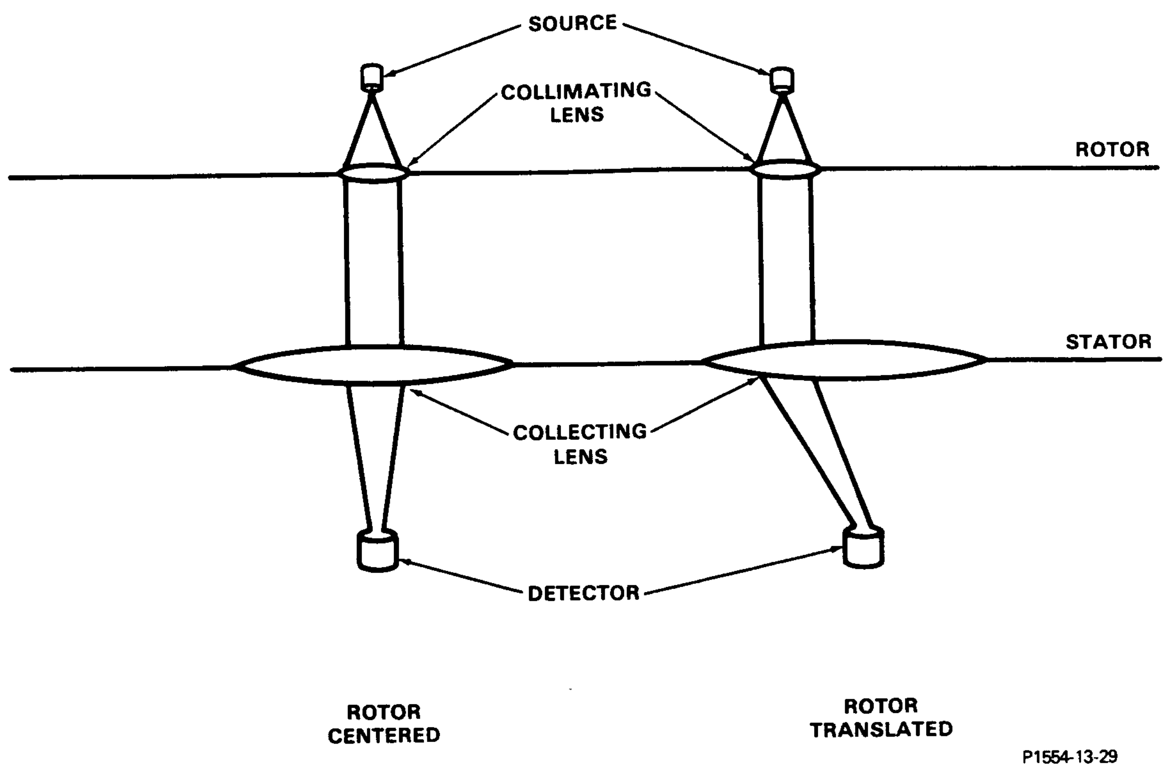

Figure 16
Optical Data Transfer Approach

BIBLIOGRAPHY

The following list of references spans all aspects and disciplines associated with this program. This listing has been divided into two parts, namely, (1) a chronological listing of those documents which are readily available from standard sources, e.g., conference proceedings, society journals, National Technical Information Service, etc; and (2) a similar list of project reports available from Flight Systems in Phoenix, Arizona. The order of listing does not reflect the relative importance of an individual report. However, the more important documents have been referenced in the test by number.

Published Documents

1. Anderson, W.W. and Joshi, S.M. The Annular Suspension and Pointing (ASP) System for Space Experiments and Predicted Pointing Accuracies; NASA TR R-448, December 1975.

2. Space Shuttle Experiment Pointing Mount (EPM) Systems, An Evaluation of Concepts and Technologies. Jet Propulsion Lab, Pasadena, California; JPL Report No. 701-1, April 1, 1977.

3. Anderson, W.W. and Groom, N.J. Magnetic Suspension and Pointing System; U.S. Letters Patent No. 4,088,018; May 9, 1978.

4. Cunningham, D.C., Gismondi, T.P., and Wilson, G.W. "System Design of the Annular Suspension and Pointing System (ASPS)"; AIAA paper 78-1311, Palo Alto, California, August 1978.

5. Anderson, W.W., and Groom, N.J. Magnetic Suspension and Pointing System; U.S. Letters Patent No. 4,156,548, May 29, 1979.

6. Anderson, W.W., Groom, N.J., and Woolley, C.T. "Annular Suspension and Pointing System"; Article No. 78-1319R, Journal of Guidance and Control, Vol 2, No. 5, September 1979.

7. Keckler, C.R., et al. Determination of ASPS Performance for Large Payloads in the Shuttle Orbiter Disturbance Environment; NASA TM-80136, October 1979.

8. Van Riper, R.V. A Precision Pointing System for Shuttle Experiment Payloads; 17th Space Congress, May 1980.

9. Hamilton, B.J. Laboratory Evaluation of the Pointing Stability of the ASPS Vernier System; NASA CR-159307, June 1980.

10. Cunningham, D.C., et al. Design of the Annular Suspension and Pointing System (ASPS); NASA CR-3343, October 1980.

11. Hamilton, B.J. "Experiment Pointing with Magnetic Suspension"; SPIE Paper 265-13, Los Angeles Technical Symposium, February 1981.

12. Van Riper, R.V. "High Stability Shuttle Pointing System"; SPIE Paper 265-12, Los Angeles Technical Symposium, February 1981.

13. Hamilton, B.J. "Vibration Attenuation using Magnetic Suspension Isolation"; 1981 Joint Automatic Controls Conference, Charlottesville, VA, June 1981.

14. Hamilton, B.J. "Stability of Magnetically Suspended Optics in a Vibration Environment"; SPIE Paper 295-21, San Diego Technical Symposium, August 1981.

15. Kibler, K.S. and McDaniel, G.A. "Application of a Local Linearization Technique for the Solution of a System of Stiff Differential Equations Associated with the Simulation of a Magnetic Bearing Assembly"; NASA TN-83146, September 1981.

16. Keckler, C.R. "ASPS Performance with Large Payloads Onboard the Shuttle Orbiter"; AIAA Journal of Guidance, Control, and Dynamics; Vol. 5, No. 1, pages 32-26; January-February 1982.

17. Hamilton, B.J. "Magnetic Suspension: The Next Generation in Precision Pointing"; 1982 Rocky Mountain Guidance and Control Conference, Keystone, Colorado, February 1982.

Project Reports

18. Axial Bearing Force Distribution
11/8/77 S. Hegyl 3964.5.4-4

19. Resolver Driver Breadboard Temperature Test
12/5/77 B. Hamilton 5869.6.3-1

20. Test of Revised Magnetic Bearing Assembly Current Loop
2/9/78 T. Gismondi 5869.6.1-3

21. Pointing Stability Using the ASPS Two Degree-of-Freedom Fixture
3/5/78 T. Gismondi/D. Cunningham 3964.6.1-2

22. Sensitivity of Compensated Magnetic Bearing Assembly Force to Proximeter Gap Error
5/3/78 D. Cunningham 3964.5-1-31

23. Investigation of Pointing Errors Due to Proximeter Calibration Errors
6/26/78 T. Gismondi 3964.6.1-4

24. Magnetic Bearing Assembly Acceptance Test
7/5/78 J. Kroeger 3964.6.4-1

25. Magnetic Bearing Equivalent Circuit
9/1/78 J. Kroeger 3964.5.4-7

26. System Calibration and Tests of the ASPS Magnetic Bearing Assembly
10/19/78 T. Gismondi/B. Hamilton 3964.6.1-5

27. ASPS Fine Pointing Mode Control Loop Bandwidth and Decoupling
11/30/78 G. Wilson 3964.5.1-34

28. Sensitivity of Compensated Magnetic Bearing Assembly Force to Magnetic Hysteresis
12/15/78 D. Cunningham 3964.5.1-37

29. Attitude Quaternion Update Using Gyro Information
1/79 SCI 3964.5.1-46

30. Mass Properties of ASPS Levitated Test Hardware
2/5/79 B. Hamilton 3964.5.1-43

31. ASPS Engineering Model Radial Servo Design
2/5/79 B. Hamilton 3964.5.1-44

32. ASPS Engineering Model Pointing Servo Design
2/5/79 B. Hamilton 3964.5.1-45

33. ASPS Engineering Model Radial Servo Performance
3/1/79 B. Hamilton 3964.6.1-6

34. Magnetic Bearing Assembly Hysteresis, A.C. Degaussing Test
3/1/79 J. Kroeger 3964.6.4-10

35. ASPS Engineering Model Pointing Servo Performance
4/1/79 B. Hamilton 3964.6.1-7

36. Magnetic Bearing Assembly Hysteresis Improvement Study-Current Compensation
5/7/79 D. Cunningham/J. Kroeger 3964.6.4-11

37. Magnetic Bearing Assembly Hysteresis Improvement Study-Anneal Investigation
5/8/79 J. Kroeger 3964.6.4-12

38. ASPS Vernier Assembly Calibration
6/20/79 B. Hamilton 3964.6.1-8

39. Mass Properties of ASPS Levitated Test Hardware (Five Degree-of-Freedom)
6.26/79 B. Hamilton 3964.5.1-7

40. Five Degree-of-Freedom ASPS Engineering Model Servo Designs
6/27/79 B. Hamilton 3964.5.1-8

41. Magnetic Bearing Assembly Hysteresis Study-Improved Anneal Evaluation
8/16/79 J. Kroeger 5869.6.4-1

42. Five Degree-of-Freedom AVS Engineering Model Characterization
10/10/79 B. Hamilton 5869.6.1-4

43. Prediction of Five Degree-of-Freedom VRCS Disturbance Response
10/26/79 T. Linton 5869.5.1-9

44. Effect of Pivot Spring Constant on ASPS VRCS Test
10/26/79 T. Linton 5869.5.1-10

45. Dynamics Model for the 4-body Rigid AVS Simulation
12/28/79 J. Mohl 5869.5.1-11

46. ASPS Vernier Engineering Model Simulation
3/28/80 T. Linton 5869.5.1-14

47. Addition of Flexible Payload to Rigid AVS Simulation
4/7/80 J. Mohl 5869.5.1-12

48. Acceleration Decoupling Law for Fine Pointing Mode
4/80 J. Mohl 5869.5.1-13

49. Magnetic Bearing Assembly Related Sensor Requirements for Inertial Pointing Mode
4/8/80 J. Mohl 5869.5.1-15

50. Lab Verification of an Optical Gap Sensing Technique
8/15/80 J. Wise 5869.6.4-2

51. Tradeoffs Leading to the Selection of Quartz Force Sensor
9/15/80 J. Wise 5869.5.4-1

52. Assessment of Off-the-Shelf Load Cell Performance
10/6/80 G. Wilson 5869.6.4-3

53. Rigid 5-body Simulation for the New AVS Configuration
1/6/81 J. Mohl 5869.5.1-17

54. Limited Roll AVS Simulation Studies
1/9/81 J. Mohl 5869.5.1-18

55. Cable Stiffness Test
4/29/81 R. Self 5869.6.1-6

56. Limited Roll AVS Simulation Study II
5/22/81 J. Mohl 5869.5.1-19

57. AVS Facility Class Payload Assessment Final Report
6/81 M. Khetarpal, et al Pub No. 71-1772

58. Optic Data Link Test Results
8/18/81 R. Self 5869.6.3-4

59. Quartex Final Report
6/82 Quartex, Inc. 5869.15.10

60. Force Sensor Acceptance Tests
6/22/82 B. Hamilton 5869.15.6

61. Single Station Simulation
9/17/82 J. Kruse 5869.5.1-20

62. Single Station Tests
10/18/82 J. Mohl 5869.6.1-7

63. ASPS Flexibility Analysis
11/4/82 J. Kruse 1700.2.1

64. Noncontact Linear Position Sensor
4/83 D. Somes, J. DeJong 5869.6.4-4